European Food Research and Technology (2025) 251:2979–2992
https://doi.org/10.1007/s00217-025-04811-0

ORIGINAL PAPER

Fructosylglycine assembles into melanoidin with more glycine than glucose while heating

Ghassan Faisal Mohsin[1,2] · **Andrea Isabel Hornemann**[3] · **Franz-Josef Schmitt**[4]

Received: 20 March 2025 / Revised: 18 May 2025 / Accepted: 3 June 2025 / Published online: 24 June 2025

Abstract

In this study, melanoidins formed from fructosylglycine and heated mixtures of glycine and glucose were analyzed and compared using spectroscopic techniques including UV/Vis, FTIR, EPR, NMR, as well as elemental analysis (EA). EA revealed that melanoidin formed from fructosylglycine incorporates a higher proportion of glycine compared to melanoidin produced through the direct reaction of glycine and glucose upon heating. FTIR spectra identified carbonyl or carboxyl groups with distinct bands at ~1749–1759 cm^{-1}, contributing to the extended π-electron system observed at 170–200 ppm in NMR spectra. EPR measurements demonstrated a higher abundance of unpaired electrons in fructosylglycine-derived melanoidin. The UV/Vis, FTIR, and NMR data indicated that the backbones of fructosylglycine-derived melanoidins contain a greater number of conjugated π bonds. Therefore, we conclude that the melanoidin skeleton synthesized from fructosylglycine includes more amino acid residues, owing to enhanced activation of nitrogen in the secondary amine of fructosylglycine compared to the primary amine of glycine. EPR results further reveal a positive correlation between melanoidin absorbance spectra, the size of their π-electron system, and antioxidant activity. These findings suggest that the nucleophilic attack of glycine's amino group on glucose's carbonyl group is facilitated in secondary amines, indicating a potential pathway to enhance melanoidin formation by incorporating secondary amines during food processing.

Keywords Maillard reaction · Melanoidin · Fructosylglycine · Secondary amine · Nucleophilic attack · Glycine

Abbreviations

MR	Maillard reaction
Glc	D-Glucose
Gly	L-Glycine
ARPs	Amadori rearrangement product
FTIR	Fourier transformation infrared
CP/MAS	Cross-polarization/magic-angle-spinning
UV/Vis	Ultraviolet/visible
EA	Elemental analysis
EPR	Electron paramagnetic resonance
NMR	Nuclear magnetic resonance

Introduction

Each person consumes approximately 10 g of melanoidins daily, which are formed as a result of the Maillard reaction (MR) during food processing. Given their prevalence in daily diets, research into the structure, biological activity, and influence of melanoidins on human health is imperative [1, 2]. The MR is a crucial mechanism for generating

✉ Franz-Josef Schmitt
franz-josef.schmitt@physik.uni-halle.de

Ghassan Faisal Mohsin
dr.ghassan.f.m@uomisan.edu.iq

Andrea Isabel Hornemann
andrea.hornemann@gmx.de

1 Ministry of Education, General Directorate Vocational Education, Department of Vocational Education in Maysan, Maysan 62001, Iraq

2 Department of Food Chemistry and Analysis, Institute of Food Technology and Food Chemistry, Technische Universität Berlin, Gustav-Meyer-Allee 25, 13355 Berlin, Germany

3 Projektträger Jülich, Lützowstraße 109, 10785 Berlin, Germany

4 Martin-Luther-Universität Halle-Wittenberg, Institut für Physik, von-Danckelmann-Platz 3, 06120 Halle, Germany

thermal flavor and color in foods and was first described by French chemist Louis Camille Maillard in 1912 [3, 4]. The reaction begins with the nucleophilic addition of the amino group of an amino acid to the carbonyl group of a reducing carbohydrate, forming Schiff bases, which are followed by dehydration [5]. These Schiff bases are then converted into Amadori rearrangement products (ARPs), which are not only more stable but also contribute to the generation of new flavors, making them useful as flavor additives [6]. As the MR progresses, ARPs produce various organic acids, carbonyls, 1,2-dicarbonyls, and heterocyclic compounds [5]. Ultimately, all these Maillard reaction products (MRPs) participate in the formation of melanoidins, resulting in the complex and heterogeneous structure of these macromolecules [7–9]. Although the chemical structure of melanoidins is not fully understood, it is well-established that they are nitrogen-containing, anionic, high molecular weight molecules with a brown to dark brown color [3, 5, 10–12]. The aldol reaction is widely discussed as a key mechanism for C-C bond formation in melanoidins [7–8], while dehydration reactions lead to the formation of conjugated double-bond systems that serve as chromophores [13]. Furthermore, in food-derived melanoidins, other food constituents such as proteins, polysaccharides, and phenolic compounds are often bound to the melanoidin structure, further contributing to its complexity [14–15].

In this work, we synthesized melanoidin from glycine (Gly) to compare the results with our former studies on melanoidins containing alanine [5, 16]. The melanoidin polymer is prepared directly from fructosylglycine and compared to a reaction starting from pure glucose (Glc) and Gly. The purpose of the study is to compare the direct formation of melanoidins from sugar and amino acids on the one hand, and the formation of melanoidins from the pure Amadori intermediate with a known chemical composition on the other hand.

Even though these two formation pathways partially overlap Yaylayan & Kaminsky presented results allowing the conclusion that melanoidin synthesized from glucose and glycine might not be identical to the melanoidin polymer formed directly from fructosylglycine [11]. They found polymeric structures formed from the Amadori intermediate and further sugar degradation after release of glycine that do not include nitrogen in the skeleton, while another pathway forming melanoidin polymer from the Amadori intermediate contains nitrogen in its structure. Cämmerer and Kroh [17] showed that melanoidin formed from glucose and glycine under solvent-free reaction condition contains sugar: amino acid in a ratio of 2:1, a result we could confirm for glucose and alanine [13, 16]. Therefore, there is a need to clarify the fate of the amino acid and consequently the nitrogen content in the polymers in more detail.

The study presented here shows that the fructosylglycine-derived melanoidin skeleton is characterized by a high nitrogen content and a darker hue, which are indicative of its distinct structural properties. The abundance of amino acids plays a crucial role in catalytic reactions and melanoidin formation [5]. This investigation aims to examine the impact of primary and secondary amines, as present in glycine and fructosylglycine, respectively, on the spectroscopic properties of the resulting melanoidins.

The number of free radicals in the melanoidin structure formed from fructosylglycine is examined along with the antioxidant activity of these melanoidins and compared with the radicals in melanoidins directly synthesized from glucose (Glc) and Gly. Due to the widespread abundance of sugar (glucose) in food products and the molecular simplicity of the amino acid (glycine), the melanoidin synthesized from these two substances was specifically studied.

Materials and methods

Chemicals and reagents

D-Glucose (99.5%) and dialysis cellulose tubing were obtained from Carl Roth (Karlsruhe, Germany), L-Glycine (99.5%) from Fluka (Steinheim, Germany), sodium metabisulfite from Merck AG (Darmstadt, Germany), and methanol and ammonia from VWR Chemicals (Darmstadt, Germany). Potassium bromide (KBr) was purchased from Sigma-Aldrich (Steinheim, Germany).

Preparation of melanoidin from Glc/Gly

The procedure for preparing melanoidin samples followed the method described by Mohsin et al. [13]. Glycine and glucose were mixed in a 1:1 molar ratio (7.5 g glycine and 18 g glucose) in a mortar and heated without solvent on aluminum foil at 160 °C for 10 min. The resulting solid product was then ground into a fine powder and subjected to dialysis. The dialysis tubing (Spectrum Por, Carl Roth, Germany) had pore sizes ranging from 1.5 to 3.0 nm, a thickness of 23 nm, and a width of 33 mm, with a molecular weight cut-off (MWCO) of 12–14 kDa. For batch dialysis, 5 g of melanoidin powder was dissolved in 300 mL of ultrapure water, and the water was replaced every 10 h, with the total dialysis time amounting to approximately 136 h. Upon completion, all melanoidin specimens were frozen and freeze-dried.

Synthesis of fructosylglycine

Fructosylglycine was synthesized following the method for fructosylalanine outlined by Mohsin et al. [16]. A mixture

of 0.28 mol glucose, 0.07 mol glycine, and 0.04 mol sodium metabisulfite was dissolved in 80 mL of methanol and 80 mL of water (v/v). The solution was refluxed for 6 h. After the reaction, fructosylglycine was isolated using a DOWEX 50WX8 cation-exchange resin. A rotary evaporator was utilized to eliminate ammonia from the solvent. After isolation, thin-layer (TLC) and high-performance thin-layer chromatography (HPTLC) chromatography techniques were applied to confirm that the isolated sample was fructosylglycine.

Preparation of melanoidin from fructosylglycine

An aluminum plate containing 25 g of fructosylglycine was heated to 160 °C for 10 min in a solvent-free environment. The resulting melanoidin was subsequently dialyzed using the same procedure previously described for melanoidin formed from heated Gly/Glc mixtures. This involved dissolving the melanoidin in distilled water and performing batch dialysis with a MWCO of 12–14 kDa, with a total dialysis time of approximately 136 h. After dialysis, the melanoidin samples were frozen and freeze-dried.

FTIR spectroscopy equipment and data capture

Fructosylglycine and melanoidins were analyzed using the same FTIR analytical parameters as described by Mohsin et al. [13]. The analysis was performed using a 1282-pixel FPA (Focal Plane Array) detector (pixel size 3 µm at 15x magnification) on the IR microscope Hyperion 3000 (Bruker Optics GmbH, Germany). Fourier transform infrared (FTIR) spectra were collected from 1.0 mg of fresh, freeze-dried samples, which were mixed with 200 mg of potassium bromide (KBr). The spectra were recorded over a wavenumber range of 3900–900 cm^{-1} with a resolution of 4 cm^{-1}.

NMR spectroscopy equipment and data capture

Fructosylglycine and melanoidins were analyzed using the same NMR diagnostic settings as reported by Mohsin et al. [13]. Melanoidins derived from Glc/Gly and fructosylglycine were placed in the magic-angle spinning (MAS) probe of an Avance 400 MHz spectrometer (Bruker, Rheinnstetten, Germany) using a 4 mm NMR rotor, which was spun at 10 kHz. Data were collected over a chemical shift range of 0 to 200 ppm.

UV/Vis spectroscopy equipment and data capture

Absorption spectra of the melanoidins were obtained using a Shimadzu UV-1800 UV/Vis spectrometer (Shimadzu, Duisburg, Germany). A melanoidin specimen (1.0 mg) was dissolved in 1 mL of pH 7.4 phosphate-buffered saline (PBS) and then diluted 1:5, resulting in a final concentration of 0.2 mg/mL. The measurements were conducted over a wavelength range of 200 to 800 nm, using a PBS solution as the blank reference.

Raman spectroscopy equipment and data capture

Raman measurements were conducted following the procedure outlined by Mohsin et al. [16]. Data were collected using a Fourier-transform Raman spectrometer (RFS 100/S, Bruker) with an excitation wavelength of 1064 nm and a spectral resolution of 2 cm^{-1}, utilizing a Nd continuous wave laser with a line width of less than 1 cm^{-1}.

EPR spectroscopy equipment and data capture

EPR spectroscopy was carried out as described by Mohsin et al. [13]. For the TEAC assay, the methodology outlined by Kanzler et al. [18] was employed to assess the antioxidant capacity of the melanoidins. The assay was conducted in triplicate to account for inherent variability in the results.

Elemental analysis of melanoidin samples

Elemental analysis (EA) was performed to determine the proportions of carbon, hydrogen, and nitrogen in the melanoidin structure, following the procedure outlined by Mohsin et al. [13]. The measurements were carried out using a Flash EA 1112 Organic Elemental Analyzer (Thermo Fisher Scientific, Dreieich, Germany). This instrument enabled the quantification of carbon, hydrogen, and nitrogen content, allowing for the calculation of their respective percentages in the melanoidin samples. The amount of oxygen was calculated as the difference on the basis that the sample contains only carbon, nitrogen, hydrogen, and oxygen.

Results and discussion

UV/Vis spectra of melanoidins

Figure 1 presents the absorbance spectra of melanoidin derived from a Glc/Gly mixture (red curve) and fructosylglycine (black curve), as determined by UV/Vis spectroscopy. The absorption is notably higher for melanoidin formed from fructosylglycine compared to that formed from Glc/Gly. Both spectra exhibit a shoulder around 280 nm, likely due to the presence of heterocyclic substructures such as furans or pyrroles, which typically absorb at this wavelength [12, 16]. This characteristic absorption at 280 nm has been discussed in several studies on melanoidin-type

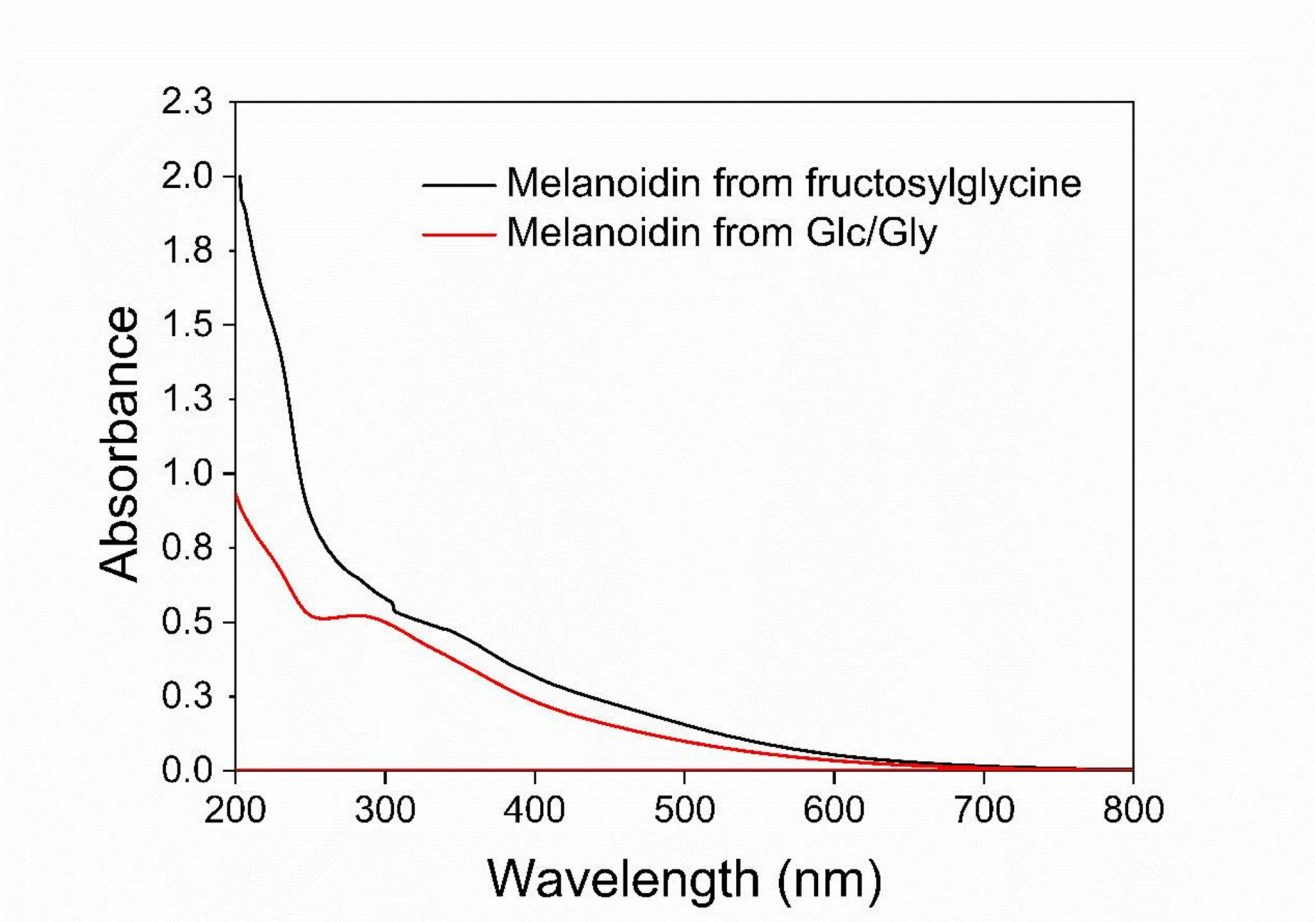

Fig. 1 UV/Vis spectra of various melanoidins

colorants [12, 16, 19–22]. Additionally, melanoidins produced from glucose and amino acid enantiomers show quite constant absorbance in the 260–320 nm range [21]. After thermal processing at 160 °C for 10 min, the fructosylglycine-derived melanoidin exhibited visibly more intense browning compared to the Gly/Glc mixture. These results suggest that the fructosylglycine-derived melanoidin contains a greater number of conjugated π bonds in its backbone and therefore a larger extended π-electron network compared to melanoidin formed from Glc/Gly.

FTIR spectra of glycine, glucose and fructosylglycine

Figure S-1a illustrates the FTIR spectrum of pure glycine, highlighting the presence of amide bands A, B, I, II, and III across different regions of the glycine backbone. Despite its importance, the significance of amide III is often overlooked in many studies. The weak signal in the amide III bands, spanning from 1380 to 1220 cm^{-1} in glycine, fructosylglycine, and melanoidin structures, offers several advantages: (i) it is not influenced by water vibrations, unlike the amide I region, (ii) it is an important characterization of different regions of proteins (generally influenced by their secondary and tertiary structure), and (iii) the bands associated with distinct secondary structures (α-helix, β-sheet, and random coils) exhibit less overlap in the amide III region compared to the amide I region [23, 24]. The amide A and amide B bands result from a resonance between amide I and N-H stretching vibrations. Amides A and B are prominently visible in glycine, while in fructosylglycine and melanoidin, these bands overlap with signals from hydroxyl groups. Glycine, in its crystalline states (α, β, γ), adopts a zwitterionic form ($+NH_3/COO^-$), a property confirmed by FTIR spectroscopy in earlier studies [10, 11, 25].

Figure S-1b presents the FTIR spectrum of pure glucose, where the νO-H stretching band around 3405 cm^{-1} and the νC-O/C-C bands near 1150 and 1023 cm^{-1} have the highest intensity. In addition, the functional groups of pure glucose in the regions 1452, 1375, 1335, 1269, and 1222 cm^{-1} are attributed to δCH, δCCH/OCH/COH, δCCH/OCH, δCH/OH, and δCH/OH, respectively [26–27]. At 1635 cm^{-1} a mode is found that can be attributed to hydroxyl groups, carbonyl/amide I, and/or water deformation.

The FTIR spectrum of pure fructosylglycine is shown in Fig. S-1c and all bands are summarized in Table S-1. A broad band from 3370 to 2500 cm^{-1} which is not resolved here can be attributed to overlapping frequencies from amide (NH^+), hydroxyl (-OH), and methyl (CH_3)/methylene (CH_2) groups and also contains contributions of Amide A and Amide B [28, 29].

The secondary amines and associated Schiff base compounds formed in fructosylglycine are evident in their crystalline structure, with a band appearing at 1628 cm^{-1}, indicating the formation of secondary structures [30]. Upon heating, these secondary amines evolve, contributing to the formation of the macromolecular structure of melanoidin. However, the specific role of secondary amines in constructing the melanoidin backbone will be detailed later. Between 1800 and 1700 cm^{-1}, the absence of absorption bands for carboxyl/carbonyl groups is notable [13]. The COOH/C=O shoulder, typically observed in deeply colored MRPs like melanoidin, is absent in the crystalline fructosylglycine.

In the 1628–1216 cm^{-1} region, bands corresponding to amides I, II, and III are present, indicating the presence of amino acid residues and peptides [29, 31, 32]. Carbohydrate contributions to the fructosylglycine structure are seen between 1150 and 1082 cm^{-1} [13]. Notably, tertiary amine groups, typically observed near 1150 cm^{-1}, are not present in the melanoidin structure [32]. A weak band around 938 cm^{-1} in the fructosylglycine spectrum is attributed to out-of-plane CH bending (δCH) (see Fig. S-1c). To have a more detailed view on the polarizable groups Raman spectra of fructosylglycine were recorded as shown in Fig. S-1d. Compared to infrared spectroscopy, Raman analysis shows weaker signals of the hydroxyl group as Raman spectroscopy is particularly sensitive to symmetric, electron-dense moieties, while infrared spectroscopy is more effective for detecting asymmetric polar groups like O-H [33]– [34]. The pronounced band observed at 2962 cm^{-1} likely corresponds to CH stretching vibrations, which are less distinct in infrared analysis (Fig. S1c) and overlap with the broad contributions of O-H.

Raman spectra also reveal a carbonyl/amide I band at 1622 cm^{-1}, with reduced intensity compared to other amide regions. Additionally, amide I and II bands are present but not as prominent (see Table S-1). Raman scattering is less effective for detecting carbohydrate-related bands in the 1148–1030 cm^{-1} range so the sugar-specific features in fructosylglycine, such as O-H, C=O, and C-O groups, are suppressed by the Raman technique.

The Raman spectra also indicate the presence of amides IV, V, and VI, characteristic of fructosylglycine's structure. These bands, along with C-H bending and νC-C stretching or wagging vibrations, are found in the range of 907 to 430 cm^{-1} [34]. Raman spectroscopy is particularly suited for analyzing the vibrational modes of nonpolar bonds such as C–C and C–H. These signals can be categorized as wagging, scissoring, rocking, or stretching modes [35].

In summary, while Raman spectroscopy is highly effective for certain molecular vibrations (e.g., C-H and C–C), it is less sensitive to polar groups such as O-H and to carbohydrate-specific signals, which are better identified by infrared spectroscopy. Thus, combining both techniques provides a more comprehensive analysis of the molecular structure of fructosylglycine.

FTIR spectra of melanoidins prepared from Fructosylglycine and Glc/Gly

The FTIR spectra of melanoidin derived from a Glc/Gly mixture (red line) and fructosylglycine (black line) are shown in Fig. 2(a) between 3900 and 900 cm^{-1}. After thermal treatment, a broad and intense band appears between 3600 and 3000 cm^{-1}, attributed to the stretching vibration of O-H groups in the melanoidin structure [36]. This is due to the multiple sugars in the melanoidin framework, contributing to numerous OH groups in different environments. Minor bands at 2935 and 2880 cm^{-1} correspond to C-H stretching vibrations. The relative intensity of the C-H absorption is correlated with the concentration of amino acids incorporated into the melanoidin and the proportion of C-H groups from amino acid components [10].

To understand the structural backbone of melanoidins, it is essential to analyze the fingerprint region between 1800 and 900 cm^{-1}. A carboxyl shoulder between 1749 and 1759 cm^{-1}, typically found in dark-colored, high-molecular-weight melanoidin, is observed in both, fructosylglycine-derived melanoidin (Fig. 2a, black line) and melanoidin from Glc/Gly mixture (red line). In addition, a stretching band at 1708 cm^{-1} broadens the spectrum associated with carbonyl groups (C=O), which may originate from carboxylic compounds (COOH) [37]– [38] or amide bonds (CO-NH_2) [39].

Amide bonds are shown to be a significant part with contributions in the key regions: amide I (1690–1600 cm^{-1}), amide II (1575–1480 cm^{-1}) and amide III (1350–1220 cm^{-1}) [5, 28, 40]– [41].

A significant absorbance band at 1627 cm^{-1} is primarily attributed to COO^-. This band has a higher amplitude in fructosylglycine melanoidin as compared to melanoidin from the Glc/Gly mixture [5, 10, 11, 16]. This band is also potentially linked to the C=O group in the D-sugar (Glc)-O-CO-(NH_2) moiety [42]. The C-O and C-C stretching vibrations, primarily from the sugar compound, are seen in the 1075 to 1035 cm^{-1} range [12, 36, 43]. In this region, the sugar bands are more intense in melanoidin from the Glc/Gly mixture compared to fructosylglycine-derived

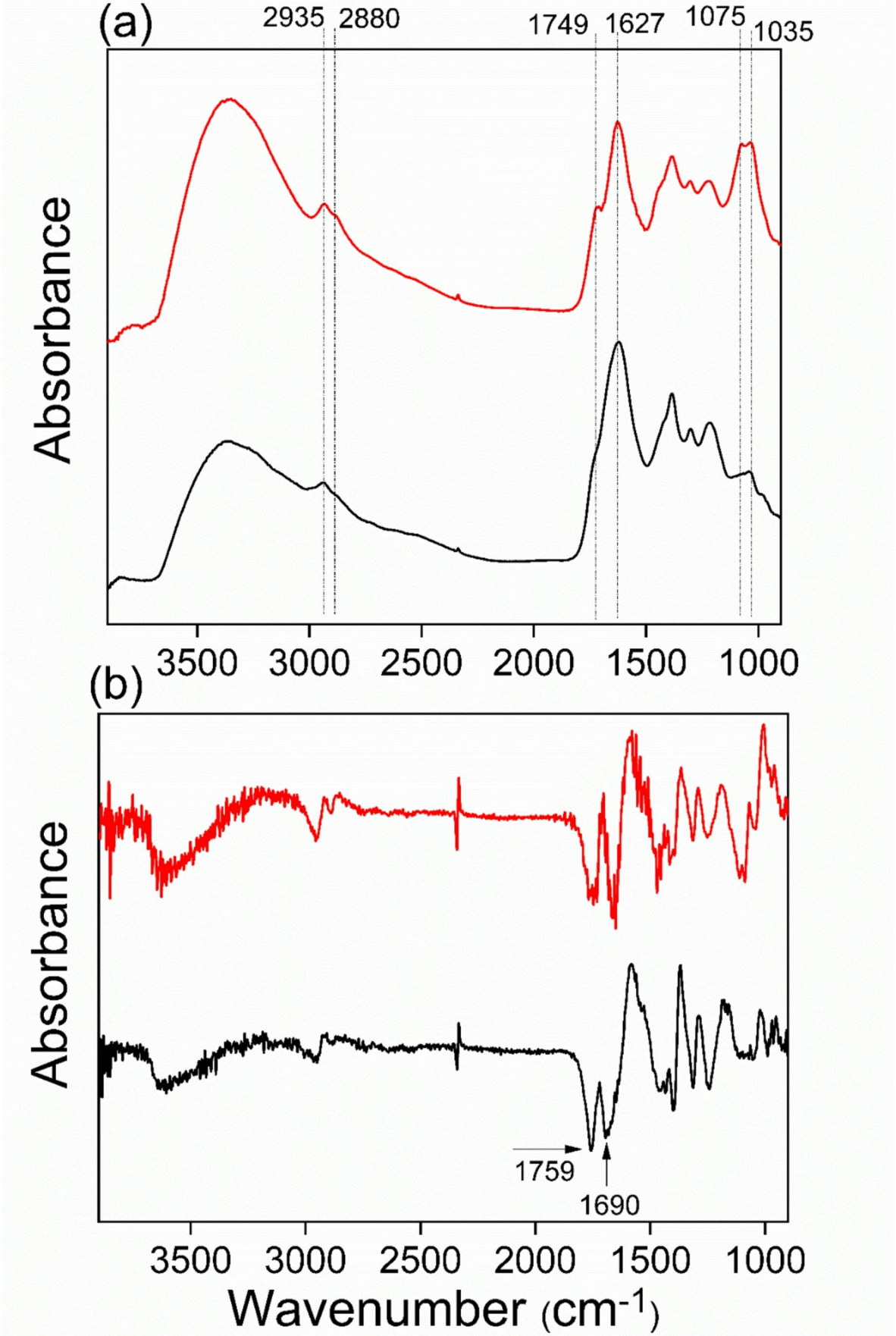
(a)
2935
2880
1749
1627
1075
1035
Absorbance
3500
3000
2500
2000
1500
1000
(b)
Absorbance
1759
1690
3500
3000
2500
2000
1500
1000
Wavenumber (cm-1)

Fig. 2 **a** FTIR spectra of melanoidin yielded from Glc/Gly mixture (red line) and melanoidin yielded from fructosylglycine (black line); **b** second derivative spectrum for Glc/Gly mixture (red line) and fructosylglycine melanoidins (black line)

melanoidin. This observation is in line with our study that compared melanoidin from Glc and alanine (Ala) with melanoidin derived from fructosylalanine, indicating that fructosylalanine and fructosylglycine form melanoidin with a higher ratio of C=O double bonds compared to C-O single bonds as found in melanoidins gained from Glc/Ala or Glc/Gly mixtures [16]. Additionally, C-H bending, indicative of saccharide bonds, appears around 950 cm^{-1} [28].

Figure 2b displays the second derivative of the FTIR data, a useful method to enhance the resolution of spectral information for understanding melanoidin structure [44]. A distinct band, representing the carbonyl or carboxyl group, is observed at approximately 1759 cm^{-1}. This analysis confirms that melanoidins derived from fructosylglycine have a relatively higher contribution from carbonyls and carboxyls than melanoidins derived from Glc/Gly mixtures. The deeper hue of fructosylglycine-derived melanoidin correlates with a higher content of carbonyl groups and larger π-electron systems compared to Glc/Gly melanoidin.

Role of secondary amines in the formation of melanoidin skeleton

Amines are classed as primary (R-NH_2), secondary (R_2NH), and tertiary (R_3N) depending on the overall number of α-carbons related to the nitrogen atom in the amine group [45]. Amines function both as bases and as reagents in nucleophilic reactions [46]. When reacted with ketones or aldehydes, secondary amines form imines or Schiff bases. In the Maillard reaction (MR), secondary amines can react with reducing sugars, leading to the condensation of the amine and carbonyl (C=O) groups, and the formation of glycosylamines. These compounds undergo further rearrangement, producing the Amadori Rearrangement Product (ARP) when a nucleophile is involved [47]. The intermediate iminium ion produced from secondary amines plays a crucial role in the later stages of the glycosylamine reaction and facilitates deprotonation, leading to the enol form of the ARP [48]. As the reaction progresses, nitrogenous polymers with a dark brown color, such as melanoidins, are formed. Notably, tertiary amines are not substrates in the MR, unlike secondary amines, which contain two α-carbons and can be linked to both saturated and aromatic carbons [45].

FTIR spectroscopy is a powerful tool for identifying secondary amines in proteins. The amide I band between 1690 and 1600 cm^{-1} is often used to evaluate protein secondary structures and conformational changes due to the C=O stretching vibrations in peptide bonds [31, 49]. The presence of secondary amines is also evident in the band at 1627 cm^{-1} [32, 50], while primary amines typically appear between 1080 and 1035 cm^{-1}. The primary amine bands can overlap with the vibration *ν*C-O/C-C. Tertiary amines are typically observed in the range between 1210 and 1150 cm^{-1}, but these bands are absent in melanoidin structures, suggesting that tertiary amines do not play a relevant role in the formation of the melanoidin backbone (see Table 1).

After heating fructosylglycine at 160 °C for 10 min, a dark brown melanoidin polymer forms. The amide I band in the 1690 to 1600 cm^{-1} range is predominantly attributed to the C=O stretching vibrations in peptide bonds [49]. In highly pigmented MRPs like melanoidins, a shoulder between 1790 and 1700 cm^{-1} is often visible [5]. The carbonyl group at 1749 cm^{-1}, thought to be associated with secondary amines [50], is critical for melanoidin polymer formation [51]. The complexity of FTIR spectra can lead to the overlap of diagnostic frequencies related to secondary structural components. The characteristic color of melanoidin polymers is attributed to chromophores, such as -C=O and -C=N, which overlap within the 1627 cm^{-1} region and contribute to the formation of an extended π-electron system within the melanoidin backbone. In conclusion, the melanoidin structure derived from fructosylglycine seems to contain more secondary amines compared to melanoidin derived directly from Glc/Gly mixtures.

^{13}C NMR spectra of melanoidins prepared from Fructosylglycine and Glc/Gly

Figure 3 presents the ^{13}C CP/MAS NMR spectra of Glc/Gly melanoidin (red line) and fructosylglycine-derived melanoidin (black line). During the intermediate and final stages of the MR, water is eliminated and aldol condensation reactions occur, leading to the formation of double bonds in both melanoidin types [16]. Therefore, we focus on the region between 100 and 180 ppm to investigate these changes. The prominent variations in the 100–160 ppm range between the NMR signals of Glc/Gly and fructosylglycine melanoidin are attributed to aromatic or olefinic carbons. The signal for sp^2-hybridized carbon atoms (chemical shift > 100 ppm) is more pronounced in fructosylglycine-derived melanoidin (black curve), suggesting a higher content of conjugated double bonds compared to the Glc/Gly melanoidin, which shows only moderate signals in this range. This indicates a relatively lower concentration of sp^2-hybridized carbons in the Glc/Gly melanoidin structure as compared to the one derived from fructosylglycine.

In the 170–200 ppm region, the signals correspond to carbonyl or carboxyl carbon atoms [5, 52], with fructosylglycine-derived melanoidin showing a robust signal, further indicating a higher content of these functional groups. The

Table 1 Functional groups of FTIR bands and 2nd derivative of FTIR spectra for melanoidin polymers

FTIR of melanoidin samples		2nd derivative of melanoidin samples	
Absorption bands	Functional groups	Minima	Functional groups
3600 − 3000	*v*O-H	3630	*v*O-H
3600 − 3000 (overlap with O-H)	$N\text{-}H^+$ Amide A/B	3600 − 3000 (overlap with O-H)	$N\text{-}H^+$ Amide A/B
2935–2880	*v*C-H_3/C-H_2	2958 − 2885	*v*C-H_3/C-H_2
1749	*v*COOH/C = O	1759	*v*COOH/C = O
1627	C = O/C = C/C = N Amide I, COO^-	1690	C = O/C = C/C = N Amide I, COO^-
1455	Amide II	1456 − 1405	Amide II
1380–1221	Amide III	1315 − 1239	Amide III
1075–1035	*v*C-O/C-C	1080	*v*C-O/C-C
950	δC-H	918	δC-H

intense coloration of the fructosylglycine melanoidin suggests an increase in aromatic content or unsaturation, contributing to an expanded delocalized π-electron system. This expanded system also might play a role in stabilizing radicals within the melanoidin structure.

These NMR findings align well with the results obtained from UV/Vis and FTIR, providing a cohesive understanding of the structural and electronic properties of fructosylglycine-derived melanoidin compared to Glc/Gly-derived melanoidin.

Elemental analysis of melanoidins prepared from Fructosylglycine and Glc/Gly

The elemental compositions of the two typical melanoidins are summarized in Table 2. The primary components of melanoidin molecules are carbon and oxygen, with hydrogen and nitrogen present in smaller amounts. The nitrogen content in the melanoidin skeleton is influenced by both the type of amino acid and the amino acid-to-sugar ratio [5, 10]. After thermal processing at 160 °C for 10 min, Glc/Gly-derived melanoidin exhibited a lower nitrogen content

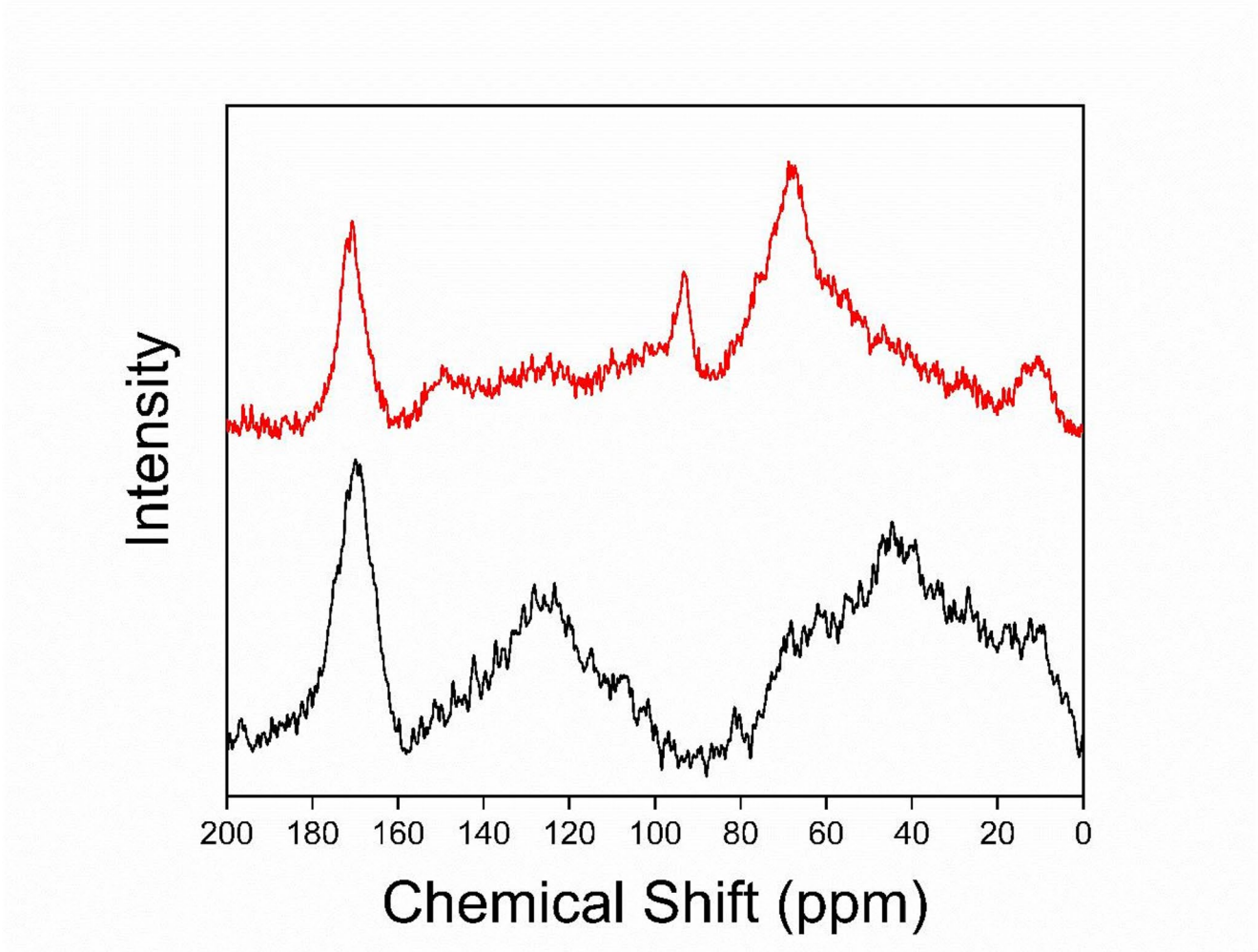

Fig. 3 ^{13}C NMR spectra of melanoidins formed from fructosylglycine (black line) and melanoidins from Glc/Gly (red line)

Table 2 Elemental compositions of melanoidins and Fructosylglycine

Substance	Weight (mg)	% *N*	% C	% H	% O*
Fructosylglycine (theoretical)		5.90	40.51	6.37	47.21
Glc/Gly melanoidin	1.29 +/- 0.02	4.02 +/- 0.02	46.46 +/- 0.05	5.77 +/- 0.02	43.76 +/- 0.10
Fructosylglycine melanoidin	1.29 +/- 0.02	9.28 +/- 0.01	46.56 +/- 0.04	5.46 +/- 0.04	38.71 +/- 0.07

*Oxygen is determined by difference

compared to fructosylglycine-derived melanoidin, in line with previous findings for Gly and Ala [5, 16].

Elemental analysis shows that melanoidin formed from fructosylglycine contains a higher amount of nitrogenous substances, indicating a greater presence of amino residues (see Table 2). In MR systems, amino acids play a critical role in triggering browning and promoting polymerization [5, 53]. Shen et al. [54] also demonstrated that increasing the amino acid content in food systems, such as bread, leads to a darker crust color and higher melanoidin formation.

EPR spectra and TEAC assay of melanoidins prepared from Fructosylglycine and Glc/Gly mixtures

Melanoidins are paramagnetic polymers that can be identified by EPR spectra due to their complex radical-containing molecular structures [5]. EPR analysis of melanoidin derived from fructosylglycine revealed a higher number of unpaired electrons compared to other melanoidin types. The antioxidant potential of different melanoidin polymers was evaluated using the Trolox equivalent antioxidant capacity (TEAC) assay, which is considered one of the most reliable methods for assessing antioxidant effectiveness [55]. Results from both the EPR and TEAC assays showed that fructosylglycine-derived melanoidin exhibited higher levels of free radicals and antioxidant activity compared to Glc/Gly-derived melanoidin (see Fig. 4a and b).

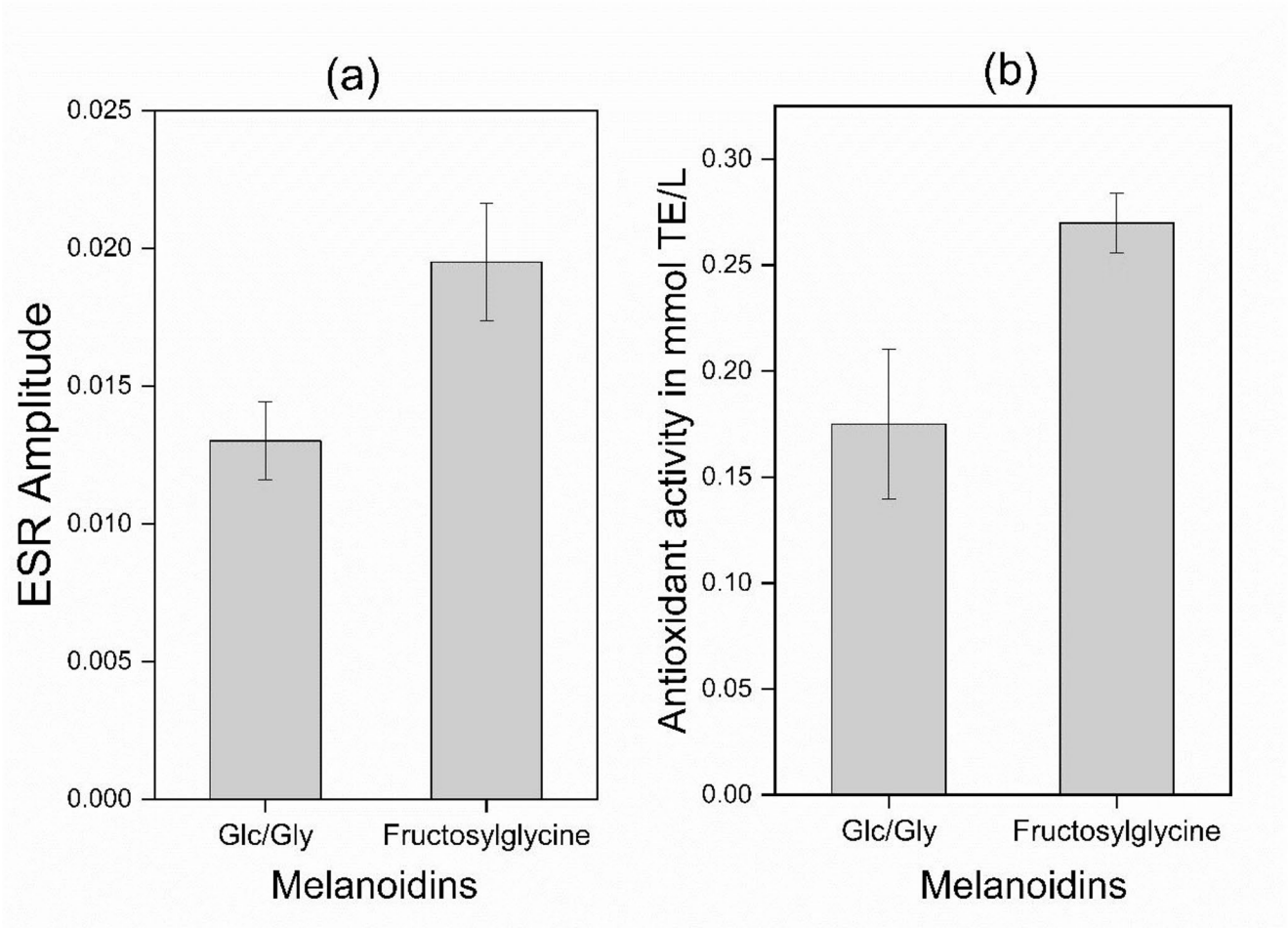

Fig. 4 **a** EPR radical signals of different melanoidin polymers; **b** TEAC assay of melanoidin samples. The mean standard deviation ($n=2$) is shown for each measurement

The high molecular weight of melanoidin polymers has been identified as a primary factor contributing to the antioxidant properties of MR systems. Several studies have confirmed that the increase in antioxidant activity correlates with color formation [56–58]. Borrelli et al. [59] found that the glucose/glycine reaction network generates a high molecular weight polymer responsible for 80% of the overall brown hue and antioxidant activity. These results suggest that the hue of melanoidins plays a crucial role in the development of their potent antioxidant capabilities, which may have significant implications for the production of safer and healthier food products in the future.

The backbone of melanoidin polymers

Various spectroscopic techniques were employed to elucidate structural attributes and molecular composition of two different melanoidin types. UV/Vis absorbance shows a higher extent of conjugated double bonds in melanoidin formed from fructosylglycine as compared to Glc and Gly mixtures. The FTIR spectra confirm that fructosylglycine-derived melanoidin incorporates more chromophores—such as conjugated C=C, C=O, and C=N bonds—compared to Glc/Gly-derived melanoidin.

NMR spectroscopy further supports this finding, showing a higher intensity of sp^2-hybridized carbon atoms in melanoidin derived from fructosylglycine. These sp^2 carbons, responsible for the formation of conjugated systems, appear predominantly in the range of 100–180 ppm.

Elemental analysis allows us to estimate the ratio of sugar molecules to amino acids in the melanoidin backbone. Shen et al. [54] and Mohsin et al. [5] demonstrated that increasing the levels of amino compounds results in a more intense browning in the final stages of the MR. Correspondingly, fructosylglycine-derived melanoidin contains a higher nitrogen content than Glc/Gly melanoidin, indicating a greater incorporation of amino residues into its structure.

Melanoidins derived from mixtures of Glc/Gly contain more sugar breakdown products generated during the initial stages of the MR. This aligns with the structural framework proposed by Cämmerer and Kroh [17] and Mohsin et al. [13, 16].

Upon heating, fructosylglycine can degrade into nitrogen-rich compounds, forming nitrogenous melanoidin structures. Yaylayan and Kaminsky [11] identified the Amadori intermediate or its derivatives as key precursors to nitrogen-containing melanoidin, with nitrogen content measured at 8.08%.

Cui et al. [60] and Yang et al. [22] suggested that the formation of products with distinct chemical compositions, along with the release of carbon dioxide (CO_2) and water (H_2O) during the Maillard reaction, could explain changes in the elemental composition of the final melanoidin products. These alterations are reflected in both the structural and chemical properties of melanoidins.

Decarboxylation and release of CO_2 occurs from the amino acid moiety in an early stage of the MR and is suggested to be the main factor for the loss of carbon [10]. The initial condensation between the sugar and the amino acid was proposed to take place through a Schiff base/imine forming possibly transient aldehyde (R-CH=O) or keto (R-C=O-R') centers that might evaporate [61].

We found that fructosylglycine dissolved in ammonia assembles into melanoidin with more than 2.3 times more nitrogen as compared to melanoidin formed from glucose and glycine (see Table 2). The nitrogen content was measured 9.3% and is significantly higher as compared to pure fructosylglycine (5.9%). This agrees with findings of Yaylayan & Kaminsky that a reaction pathway from the Amadori intermediate leads to a polymer containing 8.08% nitrogen [11]. The evaporation of CO_2 and possibly aldehydes and ketones, condensation of H_2O and remaining ammonia (even after evaporation as described in Sect. Synthesis of Fructosylglycine) can explain higher nitrogen content in the fructosylglycine-derived melanoidin structure.

Conclusions

This comprehensive study provides valuable insights into the structural and compositional properties of melanoidins derived from glucose/glycine (Glc/Gly) and fructosylglycine, highlighting the mechanisms behind their formation and distinct molecular characteristics. Using advanced analytical techniques such as elemental analysis, UV/Vis spectroscopy, FTIR, EPR, and NMR, we were able to map the key molecular signatures and structural differences between these complex MRPs.

Elemental analysis revealed substantial differences in nitrogen content between the two types of melanoidins. Fructosylglycine-derived melanoidin exhibited a significantly higher nitrogen content (9.28%) compared to Glc/Gly-derived melanoidin (4.02%). Nitrogen from residual ammonia in the solvent may also incorporate into fructosylglycine-derived melanoidin. This discrepancy emphasizes the critical role of the precursor compound fructosylglycine versus glucose/glycine in nitrogen incorporation during melanoidin formation. These results align with theoretical values and previous studies obtained from melanoidin gained from fructosylalanine and mixtures for Glc and Ala [16].

The spectroscopic analyses further highlighted the structural distinctions between the two melanoidin types. UV/Vis spectroscopy revealed characteristic shoulders around 280 nm in both melanoidins, likely attributed to heterocyclic

substructures, such as furans or pyrroles, or low molecular weight melanoidin units. However, fructosylglycine-derived melanoidin showed more intense browning, suggesting a larger and more conjugated π-electron system, which is indicative of a complex aromatic framework.

FTIR spectroscopy provided additional insights, revealing significant carbonyl and carboxyl stretching bands around 1749–1620 cm^{-1} in both melanoidins with a higher contribution in Melanoidin derived from fructosylglycine. This finding is further supported by the ^{13}C CP/MAS NMR spectra, which confirmed the presence of sp^2-hybridized carbons in the 100–160 ppm range, consistent with aromatic or olefinic character. Additionally, the robust carbonyl signals between 170 and 200 ppm in fructosylglycine-derived melanoidin further support the hypothesis of a highly conjugated π-electron system.

Amadori compounds as fructosylglycine can decompose into α-dicarbonyls like 3-deoxyglucosone (3-DG) at an early stage, which triggers the formation of advanced glycation end products (AGEs). AGEs are discussed to be responsible for the development of colorful, heterogeneous polymers like melanoidins [62]. The decomposition of the Amadori product fructosylalanine, formed from glucose and alanine, yields 3-DG-Imine and 3-DG, according to our former study [5]. We assume that 3-DG and 3-DG-Imine contribute to the synthesis of a nitrogenous polymer. It is possible to deduce that the mechanism of melanoidin formation from fructosylglycine is analogous to that of melanoidin formation from fructosylalanine and therefore can form polymeric structures rich in nitrogen.

FTIR, NMR spectra, and elemental analysis demonstrate that fructosylglycine-derived melanoidins contain more secondary amines compared to those derived from Glc/Gly mixtures. The predominant nitrogen atom in the melanoidin backbone is found in the form of secondary amines, suggesting that these amines are at least partially responsible for the intense color of fructosylglycine melanoidin.

The EPR analysis demonstrated a higher concentration of unpaired electrons in fructosylglycine-derived melanoidin, indicating a more radical-rich structure.

These findings underscore the importance of the Amadori rearrangement products in melanoidin formation, rather than direct sugar-amino acid reactions. This pathway plays a pivotal role in determining the nitrogen content and aromaticity of the final melanoidin structures, with fructosylglycine-derived melanoidin being notably richer in nitrogenous and aromatic components. Radical stabilization, in particular, contributes to the chemical resilience and antioxidant properties of these molecules.

These results suggest that fructosylglycine-derived melanoidin not only has a higher nitrogen content but also exhibits enhanced radical stabilization, which could lead to greater antioxidant benefits.

This study not only advances our understanding of melanoidin chemistry but also paves the way for future research into their biological activity and potential health benefits, given their ubiquitous presence in the human diet.

However, despite these insights, the precise mechanism underlying the formation of the brown hue and the detailed polymeric structure of Glc/Gly melanoidin remains not fully understood [63, 64]. Further research is needed to clarify the complex interactions and structural developments during the Maillard reaction.

Supplementary Information The online version contains supplementary material available at https://doi.org/10.1007/s00217-025-04811-0.

Acknowledgements The Iraqi Ministry of Higher Education and Scientific Research as well as the Ministry of Education have provided financial support, and the authors would like to express their appreciation. We appreciate the support with Raman spectra by David Buhrke and support with elemental analysis and advise from Clemens Kanzler.

Author contributions G.F.M., F.J.S. and A.I.H. conducted the experiments, G.F.M. and F.J.S. wrote the main manuscript, G.F.M. prepared the figures and tables, All authors interpreted the data and reviewed the manuscript.

Funding Open Access funding enabled and organized by Projekt DEAL. No external funding was received for the conduct, analysis, or reporting of this research.

Data availability Data will be made accessible upon request.

Declarations

Conflict of interest The authors declare no conflicts of interest related to this study.

References

1. Fogliano V, Morales FJ (2011) Estimation of dietary intake of melanoidins from coffee and bread. Food Funct 2(2):117–123. https://doi.org/10.1039/c0fo00156b

2. Yang S, Fan W, Xu Y (2022) Melanoidins present in traditional fermented foods and beverages. Compr Rev Food Sci Food Saf 21(5):4164–4188. https://doi.org/10.1111/1541-4337.13022
3. Murata M (2021) Browning and pigmentation in food through the Maillard reaction. Glycoconj J 38(3):283–292. https://doi.org/10.1007/s10719-020-09943-x
4. Shi B, Guo X, Liu H, Jiang K, Liu L, Yan N, Farag MA, Liu L (2024) Dissecting Maillard reaction production in fried foods: formation mechanisms, sensory characteristic attribution, control strategy, and gut homeostasis regulation. Food Chem 438:137994. https://doi.org/10.1016/j.foodchem.2023.137994
5. Mohsin GF, Schmitt FJ, Kanzler C, Alzubaidi AK, Hornemann A (2022) How Alanine catalyzes melanoidin formation and dehydration during synthesis from glucose. Eur Food Res Technol 248:1615–1624. https://doi.org/10.1007/s00217-022-03989-x
6. Luo Y, Li S, Ho CT (2021) Key aspects of Amadori rearrangement products as future food additives. Molecules 26(14):4314. https://doi.org/10.3390/molecules26144314
7. Kanzler C, Wustrack F, Rohn S (2021) High-Resolution mass spectrometry analysis of melanoidins and their precursors formed in a model study of the Maillard reaction of Methylglyoxal with l-Alanine or l-Lysine. J Agric Food Chem 69(40):11960–11970. https://doi.org/10.1021/acs.jafc.1c04594
8. Bork LV, Haase PT, Rohn S, Kanzler C (2022) Formation of melanoidins - Aldol reactions of heterocyclic and short-chain Maillard intermediates. Food Chem 380:131852. https://doi.org/10.1016/j.foodchem.2021.131852
9. Kitchen B, Williamson G (2024) Melanoidins and (poly)phenols: an analytical paradox. Curr Opin Food Sci 60:101217. https://doi.org/10.1016/j.cofs.2024.101217
10. Rubinsztain Y, Ioselis P, Ikan R, Aizenshtat Z (1984) Investigations on the structural units of melanoidins. Org Geochem 6:791–804. https://doi.org/10.1016/0146-6380(84)90101-3
11. Yaylayan VA, Kaminsky E (1998) Isolation and structural analysis of Maillard polymers: caramel and melanoidin formation in glycine/glucose model system. Food Chem 63(1):25–31. https://doi.org/10.1016/S0308-8146(97)00237-9
12. Kang OJ (2016) Evaluation of melanoidins formed from black Garlic after different thermal processing steps. Prev Nutr Food Sci 21(4):398–405. https://doi.org/10.3746/pnf.2016.21.4.398
13. Mohsin GF, Schmitt FJ, Kanzler C, Epping D, Flemig S, Hornemann A (2018) Structural characterization of melanoidin formed from d-glucose and l-alanine at different temperatures applying FTIR, NMR, EPR, and MALDI-ToF-MS. Food Chem 245:761–767. https://doi.org/10.1016/j.foodchem.2017.11.115
14. Moreira AS, Nunes FM, Domingues MR, Coimbra MA (2012) Coffee melanoidins: structures, mechanisms of formation and potential health impacts. Food Funct 3(9):903–915. https://doi.org/10.1039/c2fo30048f
15. Ke C, Li L (2023) Influence mechanism of polysaccharides induced Maillard reaction on plant proteins structure and functional properties: a review. Carbohydr Polym 302:120430. https://doi.org/10.1016/j.carbpol.2022.120430
16. Mohsin GF, Schmitt FJ, Kanzler C, Epping JD, Buhrke D, Hornemann A (2020) Melanoidin formed from fructosylalanine contains more Alanine than melanoidin formed from d-glucose with L-alanine. Food Chem 305:125459. https://doi.org/10.1016/j.foodchem.2019.125459
17. Cämmerer B, Kroh LW (1995) Investigation of the influence of reaction conditions on the elementary composition of melanoidins. Food Chem 53(1):55–59. https://doi.org/10.1016/0308-8146(95)95786-6
18. Kanzler C, Schestkowa H, Haase PT, Kroh LW (2017) Formation of reactive intermediates, color, and antioxidant activity in the Maillard reaction of maltose in comparison to d-glucose. J Agric Food Chem 65(40):8957–8965. https://doi.org/10.1021/acs.jafc.7b04105
19. Obretenov TD, Argirov OK, Rashkov IB (1983) On melanoidin formation with furfural participation: synthesis of melanoidins from furfural and glycine. J Food Process Preserv 7(2):105–113. https://doi.org/10.1111/j.1745-4549.1983.tb00667.x
20. Rafik M, Mas A, Elharfi A, Schue F (1997) Decoloration de solutions sucrees par ultrafiltration Sur Une membrane a base de Poly (organocyclophosphazene). Eur Polym J 33(5):679–690. https://doi.org/10.1016/S0014-3057(96)00232-7
21. Kim JS, Lee YS (2008) Effect of reaction pH on enolization and racemization reactions of glucose and Fructose on heating with amino acid enantiomers and formation of melanoidins as result of the Maillard reaction. Food Chem 108(2):582–592. https://doi.org/10.1016/j.foodchem.2007.11.014
22. Yang Y, Wang Y, Zhang Q, Chai G, Yang C, Meng Y, Xu H, Chen S (2024) Color characteristics and pyrolysis volatile properties of main colored fractions from the Maillard reaction models of glucose with three amino acids. LWT 192:115739. https://doi.org/10.1016/j.lwt.2024.115739
23. Fu F-N, Deoliveira DB, Trumble WR, Sarkar HK, Singh BR (1994) Secondary structure estimation of proteins using the amide III region of fourier transform infrared spectroscopy: application to analyze calcium-binding-Induced structural changes in calsequestrin. Appl Spectrosc 48(11):1432–1441. https://doi.org/10.1366/0003702944028065
24. Cai S, Singh BR (1999) Identification of beta-turn and random coil amide III infrared bands for secondary structure estimation of proteins. Biophys Chem 80(1):7–20. https://doi.org/10.1016/s0301-4622(99)00060-5
25. Maté B, Rodriguez-Lazcano Y, Gálvez O, Tanarro I, Escribano R (2011) An infrared study of solid glycine in environments of astrophysical relevance. Phys Chem Chem Phys 13(26):12268–12276. https://doi.org/10.1039/c1cp20899c
26. Sinyayev VA, Toxeitova GA, Batyrbayeva AA, Sassykova LR, Azhigulova RN, Sakhipov YN (2020) A comparative investigation of the IR spectra of a carbohydrate series. J Chem Technol Metall 55(4):724–729
27. Circioban D, Ledeți A, Ridichie A, Vlase T, Ledeți I, Bradu I-A, Pahomi A, Sbârcea L, Vlase G (2024) Compatibility study of Mirtazapine with several excipients used in pharmaceutical dosage forms employing thermal and non-thermal methods. J Therm Anal Calorim. https://doi.org/10.1007/s10973-024-13181-w
28. Patrignani M, González-Forte LDS (2021) Characterisation of melanoidins derived from brewers' spent grain: new insights into their structure and antioxidant activity. Int J Food Sci Technol 56:384–391. https://doi.org/10.1111/ijfs.14653
29. Ding Y, Yan C, Dai W, Wang Y, Liu S, Zheng R, Zhou X (2023) Flavor improving effects of cysteine in xylose-glycine-fish waste protein hydrolysates (FPHs) Maillard reaction system. Bioresour Bioprocess 10(1):95. https://doi.org/10.1186/s40643-023-00714-8
30. Cobb JS, Zai-Rose V, Correia JJ, Janorkar AV (2020) FT-IR spectroscopic analysis of the secondary structures present during the desiccation induced aggregation of Elastin-Like polypeptide on silica. ACS Omega 5(14):8403–8413. https://doi.org/10.1021/acsomega.0c00271
31. Usoltsev D, Sitnikova V, Kajava A, Uspenskaya M (2019) Systematic FTIR spectroscopy study of the secondary structure changes in human serum albumin under various denaturation conditions. Biomolecules 9(8):359. https://doi.org/10.3390/biom9080359
32. Nandiyanto A, Ragadhita R, Fiandini M (2023) Interpretation of fourier transform infrared spectra (FTIR): a practical approach in the polymer/plastic thermal decomposition. Indones J Sci Technol 8(1):113–126. https://doi.org/10.17509/ijost.v8i1.53297

33. Chaturvedi D, Balaji SA, Bn VK, Ariese F, Umapathy S, Rangarajan A (2016) Different phases of breast cancer cells: Raman study of immortalized, transformed, and invasive cells. Biosens (Basel) 6(4):57. https://doi.org/10.3390/bios6040057
34. Sonia, Vijayan N, Vij M, Kumar P, Singh B, Das S, Rajnikant, Soumya HN (2017) Assessment of the imperative features of an L-arginine 4-nitrophenolate 4-nitrophenol dihydrate single crystal for Non linear optical applications. Mater Chem Front 1:1107–1117. https://doi.org/10.1039/C6QM00217J
35. Segtnan VH, Hildrum KI, Wold JP (2009) 22-New methods for analysis of factors affecting meat eating quality. Woodhead publishing series in food science, technology and nutrition, improving the sensory and nutritional quality of fresh meat. Woodhead Publishing, pp 519–538. https://doi.org/10.1533/9781845695439.4.519
36. Oracz J, Zyzelewicz D (2019) In vitro antioxidant activity and FTIR characterization of high-molecular weight melanoidin fractions from different types of cocoa beans. Antioxid (Basel) 8(11):560. https://doi.org/10.3390/antiox8110560
37. Zhu J, Liu B, Li L, Zeng Z, Zhao W, Wang G, Guan X (2016) Simple and green fabrication of a superhydrophobic surface by one-step immersion for continuous oil/water separation. J Phys Chem A 120(28):5617–5623. https://doi.org/10.1021/acs.jpca.6b06146
38. Rezaeerod K, Heinzmann H, Torrence AV, Patel J, Forsythe JG (2024) Qualitative monitoring of proto-peptide condensation by differential FTIR spectroscopy. ACS Earth Space Chem 8(5):937–944. https://doi.org/10.1021/acsearthspacechem.3c00257
39. Rezvankhah A, Ghanbarzadeh B, Mirzaee H, Ahmadi Hassan Abad A, Tavakkoli A, Yarmand A (2024) Conjugation of gum Arabic and lentil protein hydrolysates through Maillard reaction: antioxidant activity, volatile compounds, functional and sensory properties. Food Sci Nutr 12(4):2855–2873. https://doi.org/10.1002/fsn3.3966
40. Ji Y, Yang X, Ji Z, Zhu L, Ma N, Chen D, Jia X, Tang J, Cao Y (2020) DFT-Calculated IR spectrum amide I, II, and III band contributions of N-Methylacetamide fine components. ACS Omega 5(15):8572–8578. https://doi.org/10.1021/acsomega.9b04421
41. Patrignani M, González-Forte LDS, Rufián-Henares JÁ, Conforti PA (2023) Elucidating the structure of melanoidins derived from biscuits: a preliminary study. Food Chem 419:136082. https://doi.org/10.1016/j.foodchem.2023.136082
42. Siemion P, Jabłońska J, Kapuśniak J, Kozioł JJ (2004) Solid state reactions of potato starch with urea and biuret. J Environ Polym Degr 12:247–255. https://doi.org/10.1007/s10924-004-8152-2
43. Ren Y, An J, Tian C, Shang L, Tao Y, Deng L (2024) Tunable physical properties of Electro-Blown spinning dextran/zein nanofibers cross-linked by Maillard reaction. Foods 13(13):2040. https://doi.org/10.3390/foods13132040
44. Yang H, Zhang Q, Zeng Y, Cheng C, Coldea TE, Zhao H (2024) Differences in structure, stability and antioxidant activity of melanoidins from lager and ale beers. LWT 205:116517. https://doi.org/10.1016/j.lwt.2024.116517
45. Smith BC (2019) Organic nitrogen compounds III: secondary and tertiary amines. Spectroscopy 34(5):22–26
46. Wang L, Ran X, Tang H, Cao D (2021) Recent advances on reaction-based amine fluorescent probes. Dyes Pigm 194:109634. https://doi.org/10.1016/j.dyepig.2021.109634
47. Szalka M, Lubczak J, Naróg D, Laskowski M, Kaczmarski K (2014) The Maillard reaction of Bisoprolol fumarate with various reducing carbohydrates. Eur J Pharm Sci 59:1–11. https://doi.org/10.1016/j.ejps.2014.04.005
48. Wirth DD, Baertschi SW, Johnson RA, Maple SR, Miller MS, Hallenbeck DK, Gregg SM (1998) Maillard reaction of lactose and fluoxetine hydrochloride, a secondary amine. J Pharm Sci 87(1):31–39. https://doi.org/10.1021/js9702067
49. Kong J, Yu S (2007) Fourier transform infrared spectroscopic analysis of protein secondary structures. Acta Biochim Biophys Sin (Shanghai) 39(8):549–559. https://doi.org/10.1111/j.1745-7270.2007.00320.x
50. Nandiyanto ABD, Oktiani R, Ragadhita R (2019) How to read and interpret FTIR spectroscope of organic material. Indones J Sci Technol 4(1):97–118. https://doi.org/10.17509/ijost.v4i1.15806
51. Mohsin GF, Schmitt FJ, Kanzler C, Hoehl A, Hornemann A (2019) PCA-based identification and differentiation of FTIR data from model melanoidins with specific molecular compositions. Food Chem 281:106–113. https://doi.org/10.1016/j.foodchem.2018.12.054
52. Hayase F, Kim SB, Kato H (1986) Analyses of the chemical structures of melanoidins by 13 C NMR, 13 C and 15 N CP-MAS NMR spectrometry. Agric Biol Chem 50(8):1951–1957. https://doi.org/10.1271/bbb1961.50.1951
53. Mikami Y, Murata M (2015) Effects of sugar and buffer types, and pH on formation of Maillard pigments in the lysine model system. Food Sci Technol Res 21(6):813–819. https://doi.org/10.3136/fstr.21.813
54. Shen Y, Tebben L, Chen G, Li Y (2019) Effect of amino acids on Maillard reaction product formation and total antioxidant capacity in white pan bread. Int J Food Sci Technol 54:1372–1380. https://doi.org/10.1111/ijfs.14027
55. Blidi S, Troise AD, Zazzaroni M, De Pascale S, Cottin S, Sturrock K, Scaloni A, Fiore A (2024) Effect of brewer's spent grain melanoidins on maillard reaction products during storage of whey protein model systems. Curr Res Food Sci. 2024;8:100767. https://doi.org/10.1016/j.crfs.2024.100767
56. Al-Farsi M, Al-Amri A, Al-Hadhrami A, Al-Belushi S (2018) Color, flavonoids, phenolics and antioxidants of Omani honey. Heliyon 4(10):e00874. https://doi.org/10.1016/j.heliyon.2018.e00874
57. Brudzyńska P, Kurzawa M, Sionkowska A, Grisel M (2022) Antioxidant activity of plant-derived colorants for potential cosmetic application. Cosmetics 9(4):81. https://doi.org/10.3390/cosmetics9040081
58. Chen W, Xie C, He Q, Sun J, Bai W (2022) Improvement in color expression and antioxidant activity of strawberry juice fermented with lactic acid bacteria: A phenolic-based research. Food Chem X 17:100535. https://doi.org/10.1016/j.fochx.2022.100535
59. Borrelli RC, Visconti A, Mennella C, Anese M, Fogliano V (2002) Chemical characterization and antioxidant properties of coffee melanoidins. J Agric Food Chem 50(22):6527–6533. https://doi.org/10.1021/jf025686o
60. Cui H, Yu J, Zhai Y, Feng L, Chen P, Hayat K, Xu Y, Zhang X, Ho CT (2021) Formation and fate of Amadori rearrangement products in Maillard reaction. Trends Food Sci Technol 115:391–408
61. Hodge JE (1953) Chemistry of Browning reactions in model systems. J Agric Food Chem 1:928–943. https://doi.org/10.1021/jf60015a004
62. Eggen MD, Glomb MA (2021) Analysis of glyoxal- and methylglyoxal-derived advanced glycation end products during grilling of Porcine meat. J Agric Food Chem 69(50):15374–15383. https://doi.org/10.1021/acs.jafc.1c06835
63. Borrelli RC, Fogliano V, Monti SM, Ames JM (2002) Characterization of melanoidins from a glucose-glycine model system. Eur Food Res Technol 215:210–215. https://doi.org/10.1007/s00217-002-0531-0

64. Comparato CN, de Araujo MN, Sakamoto IK, Fuess LT, Damianovic MHRZ, da Silva AJ (2024) Melanoidin content determines the primary pathways in glucose dark fermentation: A preliminary assessment of kinetic and microbial aspects. Fermentation 10:272. https://doi.org/10.3390/fermentation10060272